JOURNAL OF CATALYSIS **169,** 469–479 (1997)
ARTICLE NO. CA971714

Oxidative Dehydrogenation of *n*-Butane over Alkali and Alkaline Earth-Promoted α-$NiMoO_4$ Catalysts

L. M. Madeira, R. M. Martín-Aranda,[1] F. J. Maldonado-Hódar,[2] J. L. G. Fierro,* and M. F. Portela[3]

*GRECAT, Grupo de Estudos de Catálise Heterogénea, Instituto Superior Técnico, Universidade Técnica de Lisboa, Av. Rovisco Pais, 1096 Lisboa Codex, Portugal; and *Instituto de Catalisis y Petroleoquimica, CSIC, Campus UAM, Cantoblanco, 28049 Madrid, Spain*

Received November 15, 1996; revised April 3, 1997; accepted April 3, 1997

Alpha phase of $NiMoO_4$ promoted with alkaline (K and Cs) and alkaline earth (Ca, Sr, and Ba) metals has been studied for the oxidative dehydrogenation of butane. The catalysts were characterized by BET; X-ray diffraction; atomic absorption; inductively coupled plasma spectroscopy; Fourier transform infrared and Raman, X-ray photoelectron, and ultraviolet–visible diffuse-reflectance spectroscopic techniques; and CO_2 temperature-programmed desorption. The molybdate structure remains intact after doping. However, while for the Ca-, Sr-, and Ba-doped catalysts, new species were detected as oxide and peroxide compounds, only traces of alkali metals were found in the bulk of the catalysts, for the same loadings of promoter. For both catalyst series, rate of butane conversion decreases with increasing promoter content and also with increasing ionic radius of the promoter element. A decrease of surface area accounts for this trend. Catalyst surface basicity and selectivity to dehydrogenation products appear to be closely related. In fact, increased selectivity to C_4 products has been observed upon promoter incorporation, specially for K and Cs. An overdoping effect was detected for barium-doped catalysts which exhibits a maximum of basicity at 9% promoter loading. Higher levels of promoter seem to decrease the surface basicity and the C_4's selectivity. At such Ba contents the formation of three-dimensional barium compound crystallites occurs, decreasing the amount of adsorbed CO_2. Alkaline earth-promoted $NiMoO_4$ appeared to be very promising catalysts for butadiene formation, being almost twice more selective to butadiene than the undoped counterpart, for the same conversion.

1. INTRODUCTION

Olefins and aromatics are largely used as raw materials in industrial processes (1, 2). A strong market pressure compels to an increasing optimization of the present processes. Cost reduction can be obtained either by setting up new engineering concepts or by using cheaper raw materials (particularly alkanes) combined in some cases with the use of more sophisticated catalysts. In fact, in the past years, there has been a clear tendency to use light alkanes for the direct production of oxygenates via partial oxidation or for the production of olefins via dehydrogenation or oxidative dehydrogenation (ODH) due to the large availability and low price of natural gas (3, 4).

In this work we investigate the ODH of butane to olefins and butadiene. In spite of the number of reports in the literature on this matter (5–13), the optimization of the catalysts and the adequate knowledge of the factors that control selectivity and the required details of the mechanisms are still challenging problems (14–18).

Unpromoted molybdate compounds have been widely used as ODH catalysts (12, 19, 20). In the past years, alkali promoters have been used to improve the catalytic performance of molybdate systems in oxidative reactions (21–24) and some of them are even mentioned as promoters for industrial processes, in particular potassium and rubidium. It has been reported that the alkaline promoters decrease the conversion for ODH of propane in the sequence: nonpromoted $\geq$ Li > K > Rb-promoted catalysts in a particular system (V_2O_5/TiO_2 and MoO_3/TiO_2), whereas propene yields and selectivities increase at equal conversion in the same order (25). We have reported that the alkali promoters in α and β phases of $NiMoO_4$ behave similarly: reducing the catalytic activity of *n*-butane but increasing the selectivity to butenes and butadiene (21). This catalytic behavior is influenced by the concentration and basicity of promoters. The effects have been attributed to interaction of the alkali promoters with the catalyst surface. It has already been suggested that the acid–base character of the oxide ions at catalyst surface must play an important role for the ODH of butane (26, 27).

Some investigations have also been undertaken on the use of alkaline earth promoters for different processes such as oxidative coupling of methane (28, 29) or ODH reactions (13, 30–32). The use of such kind of promoters is not only related to their catalytic performances, structure, and basicity but also to their high stability. Our work is focused

[1] On leave from Departamento de Química Inorgánica y Técnica, UNED, C/Senda del Rey, s/n, 28040 Madrid, Spain.

[2] On leave from Departamento de Química Inorgánica, Facultad de Ciencias, Universidad de Granada, 18071 Granada, Spain.

[3] To whom correspondence should be addressed. Fax: 351-1-8499242.

0021-9517/97 $25.00

on the use of alkaline earth promoters on $NiMoO_4$ for the ODH of butane. A comparison between alkali and alkaline earth promoters effects was performed and the effects of promoter loading investigated.

2. EXPERIMENTAL

2.1. Catalyst Preparation and Characterization

The α-$NiMoO_4$ catalyst (with Ni/Mo atomic ratio of 1) was prepared by coprecipitation reaction, following the method described by Mazzocchia *et al.* (5), using 0.25 *M* solutions of $Ni(NO_3)_2 \cdot 6H_2O$ and H_2MoO_4. A series of $NiMoO_4$ promoted by alkaline earth metals (Ca, Sr, and Ba) and alkali metals (K and Cs) was prepared by adding 3 g of pure nickel molybdate to 30 ml of deionized water containing the appropriate concentration of dissolved alkaline or alkaline earth nitrate to obtain a promoter loading of 3% (atomic ratio metal/Mo); in the case of Ba, the loading was varied between 3 and 12%. Each resulting slurry was stirred overnight at 353 K, filtered, dried, and crushed (particle size 0.25 mm). The catalyst was then calcined in air at 823 K for 2 h prior to use.

The catalysts were characterized using appropriate techniques. BET surface area measurements were performed with a Micromeritics ASAP 2000 instrument. X-ray diffraction (XRD) patterns were recorded at room temperature with a Rigaku apparatus using the Cu $K\alpha$ radiation (Ni filter) at 2°/min. The bulk composition of the catalysts was determined by inductively coupled plasma spectroscopy (ICP) on a Perkin Elmer Plasma 400 and atomic absorption (AA) on a Perkin Elmer 4100 ZL. IR spectra of the catalysts were recorded with a Perkin Elmer 1600 FTIR spectrometer. Photoelectron spectra were acquired with a Fisons Escalab 200R spectrometer equipped with a hemispherical electron analyzer and Mg $K\alpha$ 120 W X-ray source. The powder samples were pressed into small aluminium cylinders and then mounted on a sample rod placed in a pretreatment chamber and outgassed at room temperature for 1 h. The pressure in the ion-pumped analysis chamber was below 3×10^{-9} Torr (1 Torr = 133.33 Pa) during data acquisition. The spectra were collected for 20 to 90 min, depending on the peak intensities, at a pass energy of 10 eV (1 eV = 1.602×10^{-19} J). The C1*s*, O1*s*, Mo3*d*, and Ni2*p* peaks were recorded for all the samples, and Ca2*p*, Sr3*d*, Ba3*d*, K2*p*, or Cs3*d* for the promoted samples. The intensities were estimated by calculating the integral of each peak after smoothing and subtraction of the background. All binding energies (BE) were referenced to the C1*s* line at 284.9 eV, which gave BE within an accuracy of ±0.1 eV. FT Raman spectra were obtained with a Brucker Raman spectrometer (exciting line, 1064 nm). Around 40 mW of laser output at the source was used with a spectral resolution of 4.0 cm^{-1}. UVDRS spectra were recorded with a Cary 1 ultraviolet–visible Varian spectrophotometer with a diffuse-reflectance accessory. Samples were placed in quartz cells and were scanned against a pure barium sulfate standard.

The basicity of the catalysts surface was studied by CO_2 TPD technique. A blank experiment carried out in He flow until 650°C showed that between 550 and 650°C the detector signal is negligible. Consequently, about 0.25 g of catalyst was pretreated in each experiment by heating the sample in He flow until 550°C to clean the surface, but avoiding transition to the metastable β phase which is already present at 595°C (20). After this process, the catalysts were saturated in CO_2 at 30°C, purged during 20 min in He flow, and then CO_2 was desorbed by heating at 10°C/min in a He flow of 1 cm^3/s with on-line gas analysis performed with the TC detector of a Shimadzu GC-8A gas chromatograph.

2.2. Steady-State Catalytic Activity Studies

Steady-state experiments were carried out in a fixed-bed, continuous-flow tubular quartz reactor and the products separated and analyzed using an on line Shimadzu GC-8A gas chromatograph with two columns as described elsewhere (21). The catalyst (0.3 g) was mixed with inert quartz (50–70 mesh) in a volume ratio of 1 : 4 catalyst to quartz.

The feed for these experiments was a mixture of 4% *n*-butane, 8% oxygen, and 88% nitrogen and the contact time (W/F) was 11.2 $g_{cat} \cdot h \cdot (mol_{C_4H_{10}})^{-1}$. The ODH of butane was studied in the temperature range 375–525°C at atmospheric pressure. For comparisons on equal conversion levels, the temperature was varied to keep conversion of butane constant (near 4%) for each catalyst. Blank runs showed that under the experimental conditions used in this work, the homogeneous reactions can be neglected.

3. RESULTS

The $NiMoO_4$ prepared by coprecipitation yields a yellow-green catalyst precursor, which is thermally activated for 2 h at 550°C in air flow to obtain the α-$NiMoO_4$ catalyst with a well-defined crystalline structure. Important structural differences between the precursor and the catalyst are evidenced by XRD (Fig. 1). The nature of the catalytic system required the use of a combination of complementary characterization techniques in order to understand the structural and chemical features of the catalysts. All the experimental techniques used to characterize the catalysts (XPS, ICP, AA) showed a pure nickel molybdate compound with an atomic ratio Mo/Ni = 1. Moreover, no excess of NiO or MoO_3 was recorded by XRD, FTIR, or FT Raman techniques.

Although in all cases the dopant solutions were prepared to yield dopant loadings between 3–12% (metal/Mo molar ratio), in the case of alkali metals ICP analysis detected only traces of them in the bulk, but the preparation ratio was found on the surface by XPS (21, 33). In the case

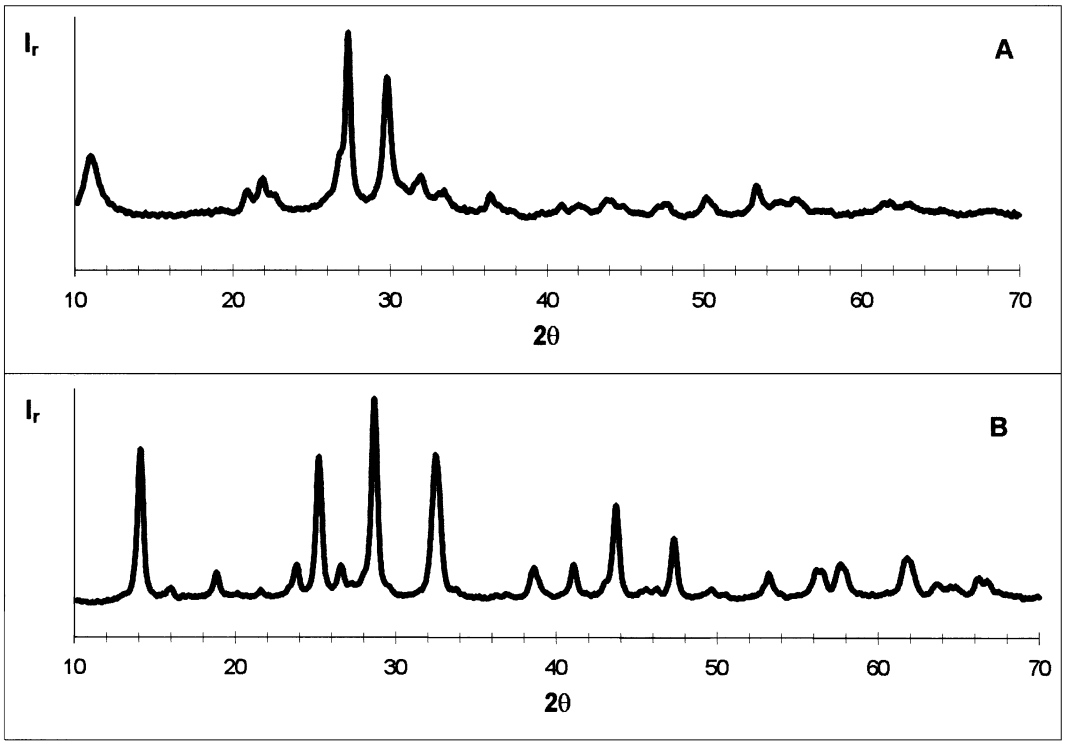

FIG. 1. X-ray diffraction patterns at 21°C of $NiMoO_4$ precursor (A) and catalyst (B).

of alkaline earth promoters the concentration corresponding to preparation was observed. The recorded results are compiled in Table 1. When comparing the effects of the different promoters it must be taken into account that along this paper the catalysts are labeled by their programmed preparation metal/Mo ratio.

3.1. Surface Area Analysis

The BET surface areas of the promoted catalysts were found to decrease with respect to the unpromoted $NiMoO_4$ (Table 1). As observed in other studies with alkali promoters (21, 25), BET area decreases as the ion size and the concentration of promoters increase. It is noteworthy that, for 3% M–$NiMoO_4$ catalysts, the alkali-promoted catalysts exhibit a smaller surface area than the alkaline earth promoted samples.

TABLE 1

BET Areas and Atomic Ratios of the Unpromoted and Promoted α-Phase Catalysts

Catalyst	S_{BET} (m^2/g)	M/Mo (ICP)	M/Mo (XPS)
$NiMoO_4$	44.1	—	—
3% K–$NiMoO_4$	33.3	Traces	0.025
3% Cs–$NiMoO_4$	28.7	Traces	0.030
3% Ca–$NiMoO_4$	37.1	0.030	0.014
3% Sr–$NiMoO_4$	36.8	0.030	0.011
3% Ba–$NiMoO_4$	35.2	0.029	0.020
6% Ba–$NiMoO_4$	36.7	0.061	0.043
9% Ba–$NiMoO_4$	35.2	0.091	0.041
12% Ba–$NiMoO_4$	26.6	0.125	0.046

3.2. X-Ray Photoelectron Spectroscopy

In order to investigate the composition of the catalyst surface, possible variations in the oxidation state, changes in the electronic density of the Ni–Mo–O system and the nature of surface species on these oxides, XP spectra were recorded.

In a previous work (21), a shift to lower binding energies was found in the Mo3*d* doublet upon alkali metal addition, suggesting an increase of the average electron density in the molybdenum atoms. No significant changes of the BE of Mo3*d*, Ni2*p*, or O1*s* were observed due to the alkaline earth promoters addition, though the BE of Ni2*p* follows the sequence: unpromoted < Ca ≅ Sr < Ba, but this trend is not corroborated in Ba-promoted catalysts with higher Ba loadings. The Mo3$d_{5/2}$ and Ni2$p_{3/2}$ BE for the unpromoted catalyst (232.6 and 856.1 eV, respectively) are typical of the Mo^{6+} and Ni^{2+} states. Quantitative XPS data are summarized in Table 1.

3.3. X-Ray Diffraction

The stability of α phase in the temperature range used for the catalytic experiments was checked by HTXRD (33). This was done comparing the patterns obtained at ambient temperature and 625°C.

As already reported, the X-ray diffraction patterns recorded for the alkali-promoted molybdates revealed no changes when compared with the unpromoted α-$NiMoO_4$ (21, 33), showing the characteristic principal line at $2\theta = 28.7^\circ$ (ASTM, 33-948). The same results were obtained for the 3% alkaline earth-doped catalysts. Special mention must be made about the Ba-doped catalysts in which two different species, barium oxide and barium peroxide, are present. The X-ray diffraction patterns of Ba-doped catalysts at different promoter loadings show that BaO and BaO_2 species increase as the Ba content increases (Fig. 2) (BaO, ASTM, 22-1056: 27.8°_{100}, 32.3°_{86}, 46.3°_{49}, 54.9°_{32}; BaO_2, ASTM, 7-233: 26.7°_{100}, 42.6°_{50}, 46.3°_{45}, 69.6°_{6}). The remaining peaks coincide with those of the α-$NiMoO_4$ diffractogram.

3.4. FTIR

The FTIR spectrum of the unpromoted $NiMoO_4$ agrees with literature (20, 34) (Fig. 3). Alkali-doped catalysts did not show significant changes with respect to α-$NiMoO_4$. The addition of Ca, Sr, and Ba yields two new bands located near 815 and 875 cm^{-1} (Fig. 3). Moreover, the first band shifts to higher frequencies according the sequence Ca (802) < Sr (814) < Ba (817). These bands are also observed in Fig. 4 where the influence of promoter contents is shown. It appears that an increase in Ba concentration leads to an increase of intensity of both bands.

Although carbonates exhibit bands with medium intensity in the range 800–880 cm^{-1} (35), carbonates must be ruled out because the characteristic bands, of very strong

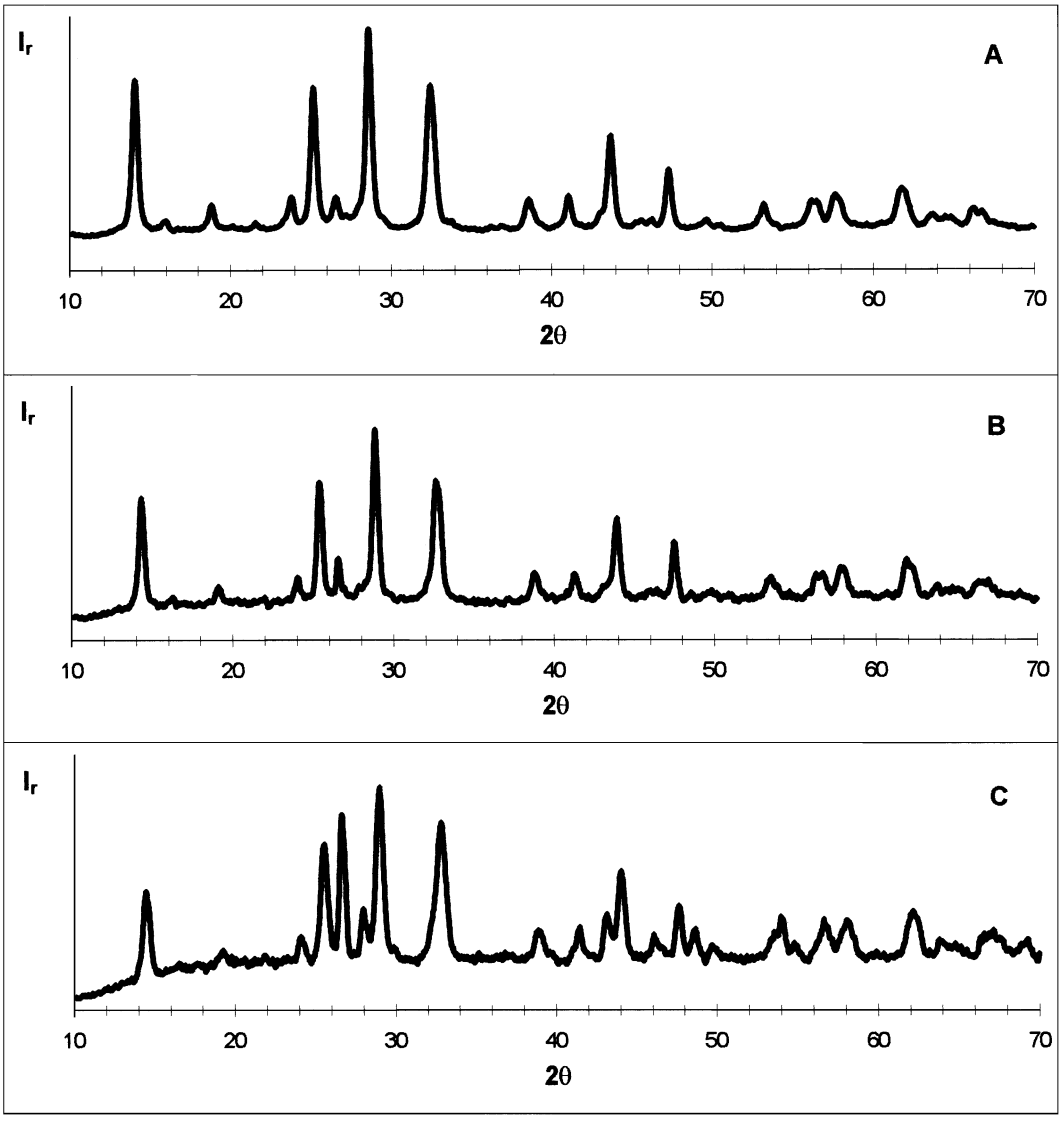

FIG. 2. X-ray diffraction patterns at 21°C of unpromoted (A) and Ba-promoted α-$NiMoO_4$: 3% (B) and 12% (C).

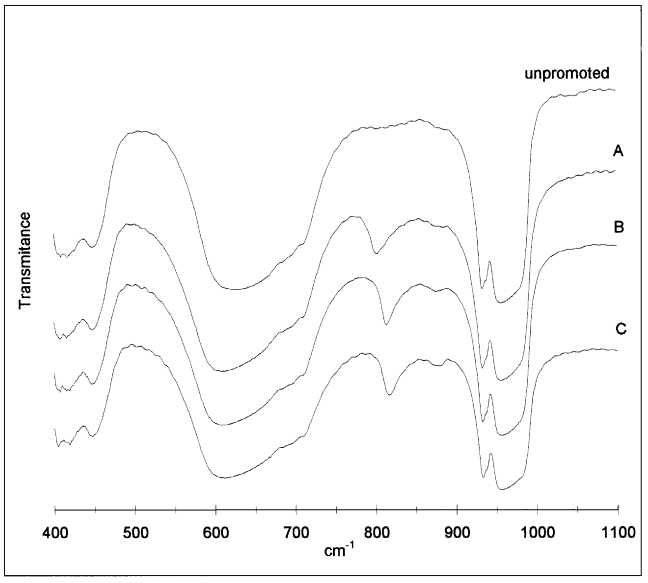

FIG. 3. FTIR spectra of unpromoted and promoted α-$NiMoO_4$: 3% Ca (A), 3% Sr (B), and 3% Ba (C).

intensity between 1410 and 1450 cm^{-1} (not shown in the figures), are absent. It is likely that they are associated to O_2^{2-} ions, which usually display ν_{O-O} vibrations between 800 and 900 cm^{-1} (36). The existence of such species could affect the catalytic behavior of the studied catalysts.

3.5. FT Raman Spectroscopy

Raman spectroscopy is a particularly powerful technique for determining small amounts of segregated phases, especially MoO_3 in the Ni–Mo–O system. Raman spectroscopy

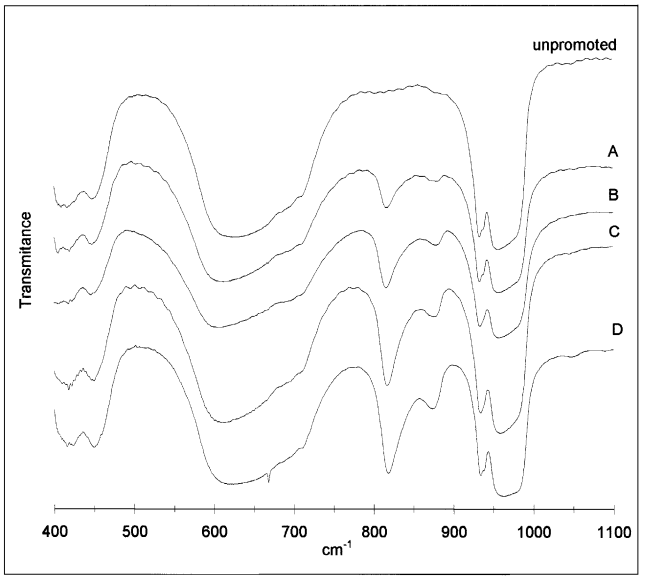

FIG. 4. FTIR spectra of unpromoted and Ba-promoted α-$NiMoO_4$: 3% (A), 6% (B), 9% (C), and 12% (D).

TABLE 2

Raman Bands (cm^{-1}) of $NiMoO_4$ and MoO_3 (6)

Sample								
$NiMoO_4$	963 vs	916 s	709 s	494 m	420 m	389 m	373 m	179 m
MoO_3	998 s	822 vs	670 s	381 m	339 m	293 m	285 s	160 m

characterization of $NiMoO_4$ has been reported previously (6). The sharp Raman peaks of nickel molybdate and MoO_3 are listed in Table 2. As described by Mazzocchia *et al.* (5), nickel molybdate catalysts containing an excess of Ni (which stabilizes the metastable β-phase) present new bands in the IR spectrum at room temperature (800, 880 cm^{-1}), but the Raman spectrum is the one characteristic of $NiMoO_4$. However, catalysts with an atomic ratio Mo/Ni > 1 exhibit additional bands either in the IR spectrum (990, 860, 810 cm^{-1}) or in Raman, typical of MoO_3. Figure 5A displays the Raman spectra of the stoichiometric $NiMoO_4$ sample which shows three characteristic bands at 962, 913, and 707 cm^{-1}. No Raman bands of free MoO_3 phase were detected for our prepared $NiMoO_4$.

Raman bands at around 965–944, 880, 390, and 240–210 cm^{-1} are consistent with octahedrically coordinated polymolybdates (37, 38). A Mo–O–Mo deformation mode band at around 260–230 cm^{-1} and the band at around 390 cm^{-1} could be associated with the Mo–O bending mode. The major feature is the Mo–O stretching mode at around 962 cm^{-1}.

To examine whether peroxide ions were indeed present in the Ba/$NiMoO_4$ catalysts, a Raman spectrum was recorded for the 12% Ba-doped catalyst. Raman spectroscopy is particularly suitable for this purpose because the O–O stretching mode in peroxide ions is Raman active. The spectrum of the barium-doped sample (Fig. 5B) is similar to that recorded for the pure $NiMoO_4$ showing no shifts of the bands, but new peaks appeared at 891 and 837 cm^{-1}. According to the literature, a strong peroxy stretching line occurs in the Raman spectrum at 890 cm^{-1} (39). The second peak in the 12% Ba–$NiMoO_4$ catalyst is also due to O_2^{2-} ions because the spectrum of pure BaO_2 yields, besides minor bands at 829 and 821 cm^{-1}, an intense band at around 842 cm^{-1} (39–41) which is assigned to symmetric O–O stretching vibrations.

It is noteworthy that no carbonate species were detected in the Raman spectrum of the barium-doped catalyst because no bands appeared at 1055 or 689 cm^{-1} which are assigned to modes of CO_3^{2-} ions (40, 41).

3.6. Ultraviolet-Visible Diffuse Reflectance Spectroscopy

The ultraviolet–visible diffuse-reflectance spectrum of pure α-$NiMoO_4$, displayed in Fig. 6, shows a maximum at around 215 nm and a shoulder near 300 nm, suggesting the

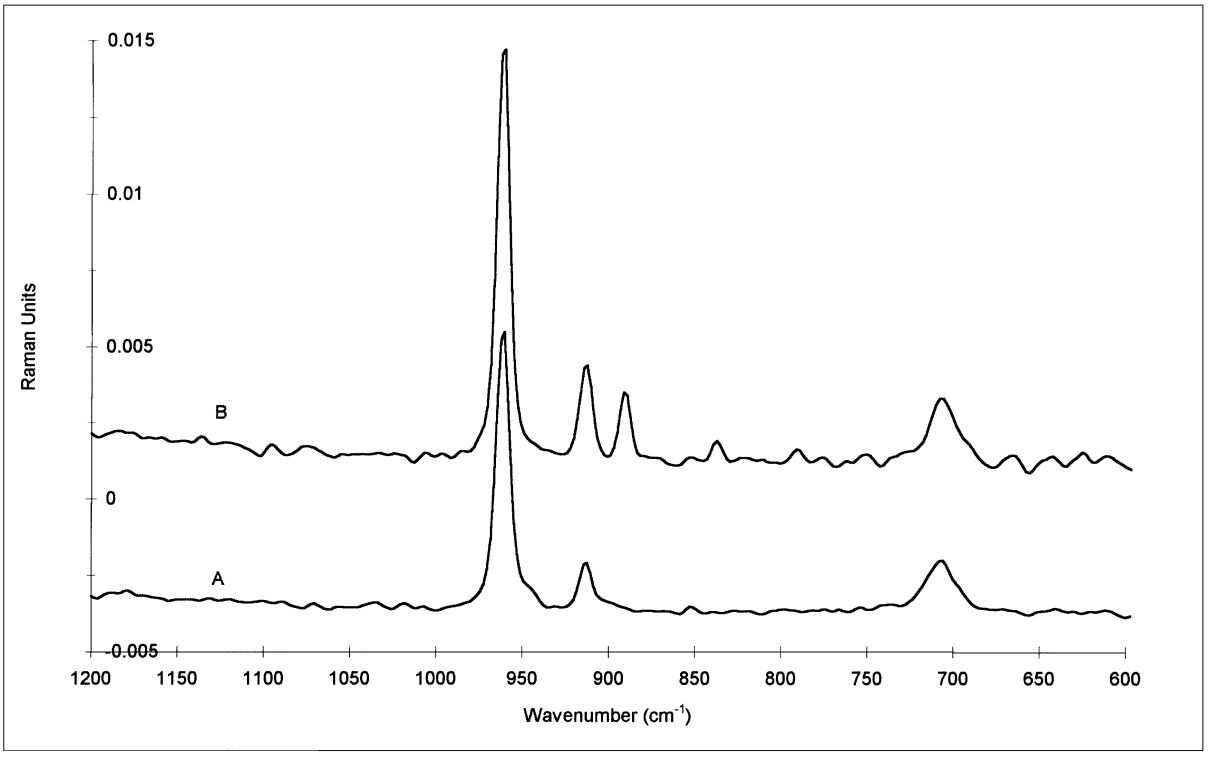

FIG. 5. Raman spectra of pure α-$NiMoO_4$ (A) and 12% Ba–α-$NiMoO_4$ (B).

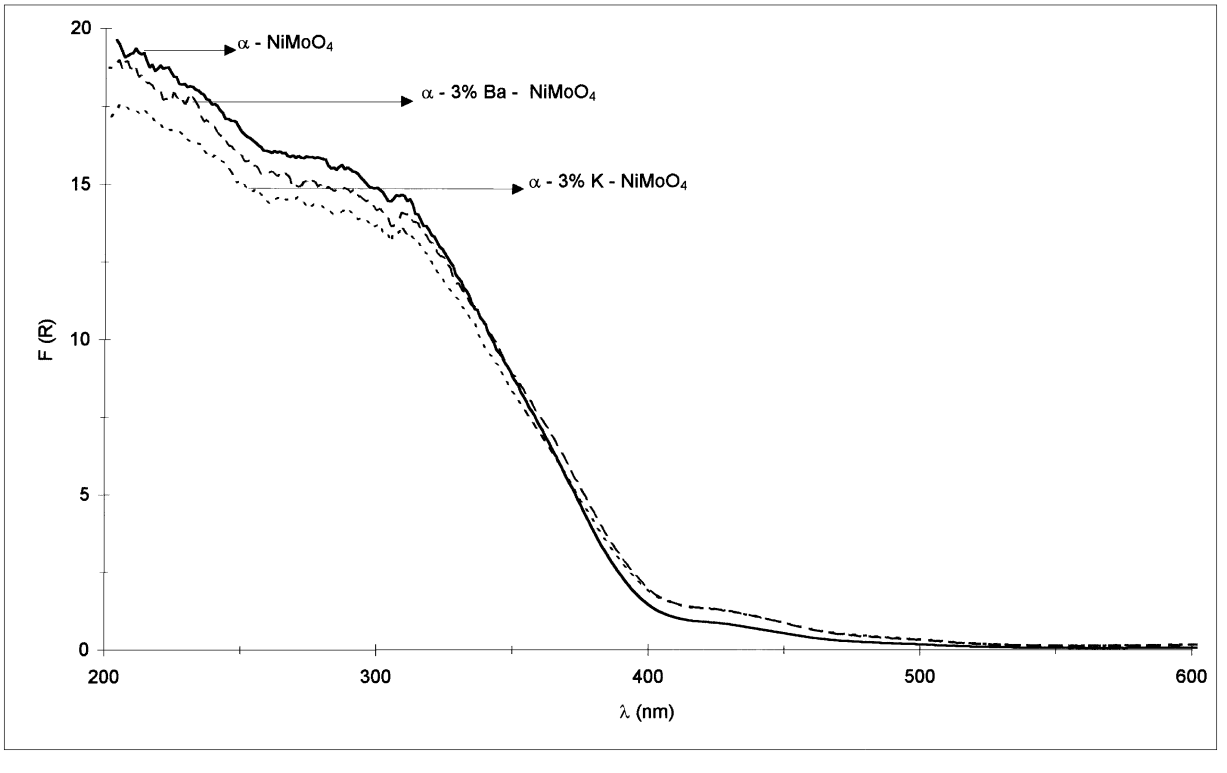

FIG. 6. Ultraviolet–visible diffuse-reflectance spectra of α-$NiMoO_4$, 3% Ba–α-$NiMoO_4$, and 3% K–α-$NiMoO_4$.

presence of two Mo–O symmetry environments. The common use of UVDRS to determine the local symmetry of supported molybdenum cations has been reviewed (42). As mentioned by Williams *et al.* (37), UVDRS, without supplementary evidence, is ineffective for differentiating tetrahedrally (T_d) and octahedrally (O_h) coordinated molybdenum because the two absorption bands observed in the electronic spectra are inconsistent with the FT Raman results which evidenced that only Mo(O_h) was present. The broad nature of electronic absorption bands ill-characterized and the use of different reference compounds and instrumentation have led to contradictory UV results. Traditionally, absorption bands from 250 to 280 nm have been assigned to Mo(T_d) and bands from 300 to 330 nm were assigned to Mo(O_h) (42). However, Williams *et al.* (37) observed absorption bands of compounds containing octahedrally coordinated molybdenum not only at around 325–330 nm but also near 230 and 280–295 nm. They assigned those bands to Mo(O_h) according to Raman data.

Considering the literature information, the possible interpretation of the UVDR spectrum (Fig. 6) is to assume that the band at 215 nm and the shoulder near 300 nm are due to Mo(O_h). This interpretation is supported by the structural data of $NiMoO_4$ α-phase (5, 20) and by the Raman and FTIR results reported above. The addition of alkali and alkaline earth promoters does not alter significantly the $NiMoO_4$ UVDR spectrum (Fig. 6).

3.7. Temperature-Programmed Desorption of CO_2

The basicity of the catalyst surface was examined by CO_2-TPD. The existence of two types of active sites with very different basicity has been evidenced in the unpromoted catalyst which exhibits two maxima, one at 275°C and the second one starting about 525°C. The precise position of the latter could not be accurately defined to avoid the α- to β-phase transition (Fig. 7A).

Total amount of adsorbed CO_2 increases upon addition of 3% Cs to $NiMoO_4$ (Fig. 7A), in agreement with previous results (33), and the maximum of the first desorption peak is shifted to lower temperatures. The CO_2-TPD profile for 3% Ba–$NiMoO_4$ does not evidence significant changes in the strength of the nickel molybdate sites, but exhibits a slight higher basicity (Fig. 7A). The higher basic character of alkali promoters is quite nicely illustrated in Fig. 7A by the larger area of the 3% Cs–$NiMoO_4$ curve. It must be emphasized that for the more basic sites, catalyst doping with cesium or barium does not affect significantly their strength and number.

The influence of barium loading of nickel molybdate on CO_2-TPD results is presented in Fig. 7B. Any increase in Ba contents up to 9% increases the total basicity of the catalysts. But although the number of basic sites increases with Ba loading, it appears that such sites become progressively weaker. However, for the 12% Ba–$NiMoO_4$, there is a decrease in the total basicity with respect to the 9% Ba sample. Such overdoping effect was also observed for Cs-doped catalysts (33), which display a maximum of adsorbed CO_2 for 3% Cs–$NiMoO_4$.

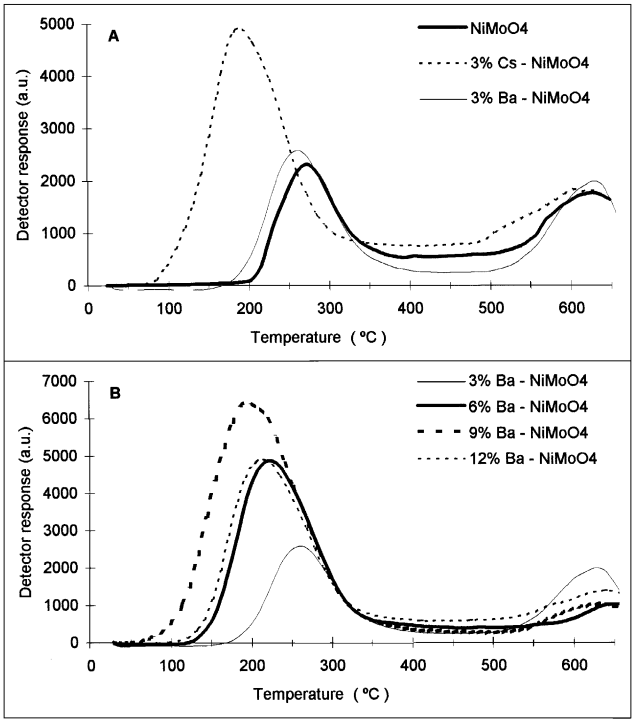

FIG. 7. CO_2-TPD of unpromoted and 3% promoted α-$NiMoO_4$ (A) and of Ba-doped catalysts (B).

3.8. Steady-State Experiments

Butane ODH was tested on unpromoted and 3% alkaline earth (Ca, Sr, and Ba) promoted α-$NiMoO_4$ catalysts. In order to investigate the effect of the promoter nature, experiments were also performed with two alkali-doped catalysts: 3% K and 3% Cs–$NiMoO_4$. The effect of the promoter concentration was studied by varying the Ba contents from 3 to 12%. The observed reaction products were CO, CO_2, 1-butene, 2-*trans*-butene, 2-*cis*-butene, and butadiene and no oxygenated organic compounds were detected. The absence of such compounds was also found over Mg–V–O systems and this fact was attributed by Chaar *et al.* (13) to the basicity of these materials, which favors the rapid desorption of the olefins formed and limits the consecutive oxidation to maleic anhydride or to other oxygen-containing compounds.

The activity of the tested 3% M–$NiMoO_4$ catalysts shows a decrease with respect to the unpromoted catalyst which is more intense with the K- and Cs-doped samples (Fig. 8).

Furthermore, the product distribution changes by effect of alkaline earth promoters, showing an improvement in the selectivity to dehydrogenation products (C_4's), which

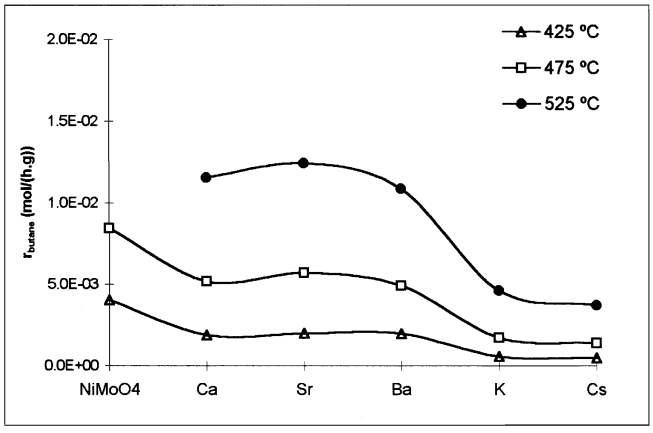

FIG. 8. Rates of butane conversion on unpromoted and 3% promoted α-$NiMoO_4$ at different temperatures (feed mixture of 4% n-C_4H_{10}, 8% O_2, and 88% N_2 at $W/F = 11.2\ g_{cat} \cdot h \cdot (mol_{C_4H_{10}})^{-1}$).

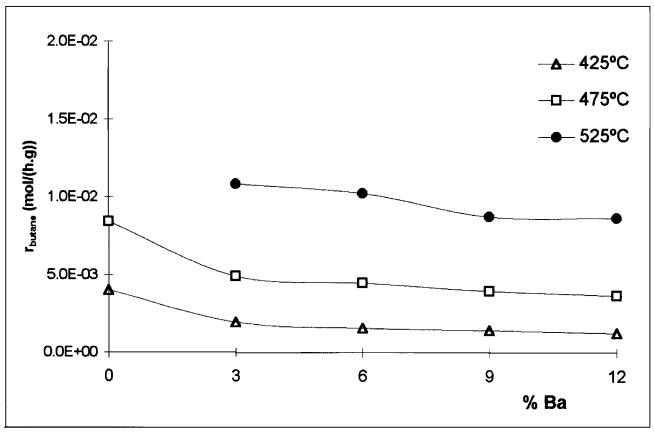

FIG. 10. Influence of barium contents on rates of butane conversion at different temperatures (same reaction conditions as Fig. 8).

increases from around 60% for the unpromoted catalyst to ≅70% for Ca-, Sr-, and Ba-promoted ones at constant conversion of 4% (Fig. 9A). The increase of the C_4's selectivities is due principally to the large formation of butadiene obtained with alkaline earth-promoted catalysts. The butadiene selectivity increases almost twice with respect to the unpromoted catalyst, showing at 4% conversion a selectivity of 16% for the unpromoted catalyst and between 28 and 30% for the promoted ones (Fig. 9B). If we compare the results obtained with alkali (K and Cs) and alkaline earth doped catalysts, it is clear that alkali promoters lead to a greater increase of C_4's formation (Fig. 9A), but the butadiene selectivities are lower, at equal conversion levels (Fig. 9B).

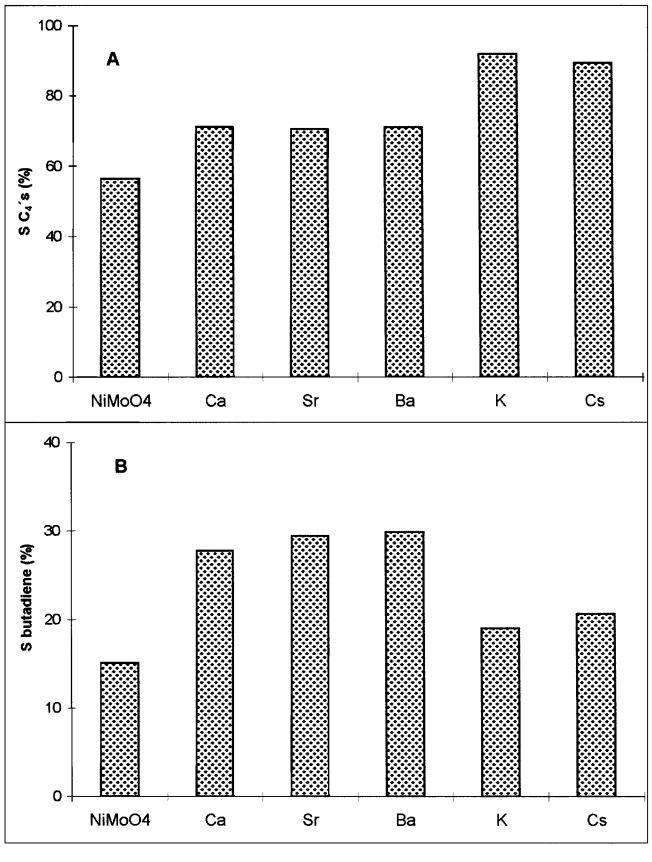

FIG. 9. Selectivity to dehydrogenation products (A) and butadiene (B) at equal conversion levels (4%) on unpromoted and 3% promoted α-$NiMoO_4$ (same reaction conditions as Fig. 8).

The influence of the promoter loading was tested varying the Ba concentration between 3 and 12% (in surface between 2.0 and 4.6%, Table 1). Figure 10 shows that rate of butane conversion decreases as the Ba concentration increases and these results are again in agreement with the evolution of the BET surface areas (Table 1). If activities are based on unity surface area (mol/(h · m^2)), the different rates of butane conversion must originate from the different nature of the catalysts surface. In this way, the more basic catalysts will present smaller activities because the butane–surface interactions are weakened. In fact, the introduction of promoters with basic character in $NiMoO_4$ decreases the activity, specially for alkali metal doping (Fig. 11A). In the same way, the influence of barium loading on normalized activity shows that up to 9% concentration of promoter the activity decreases, being however slightly higher for the 12% Ba–$NiMoO_4$ catalyst (Fig. 11B). This fact goes in parallel with the decrease of basicity of such catalyst, as evidenced by CO_2-TPD (Fig. 7B).

With respect to the products distribution, the C_4's selectivity (Fig. 12) shows an important improvement up to 9% Ba–$NiMoO_4$. Increasing the Ba contents, the C_4's selectivity remains higher than the one found for the unpromoted catalyst but decreases with respect to the catalysts doped with lower Ba concentrations. The butadiene selectivity shows a similar behavior (Fig. 12). The catalyst with 9% of Ba is twice more selective for butadiene than the undoped nickel molybdate at 4% conversion.

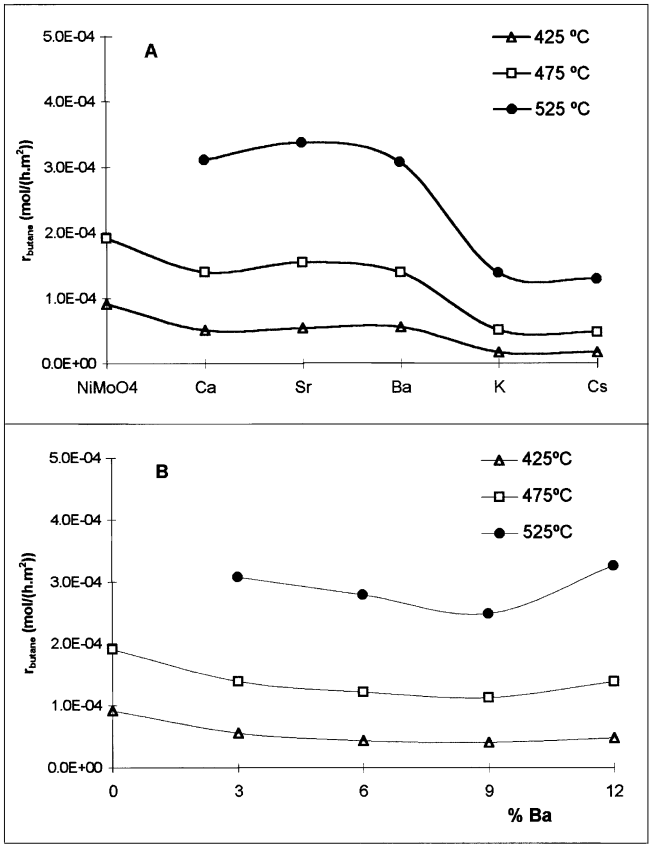

FIG. 11. Normalized rates of butane conversion on unpromoted and 3% promoted α-$NiMoO_4$ (A) and on barium-doped catalysts (B) at different temperatures (same reaction conditions as Fig. 8).

4. DISCUSSION

According with the ICP and XPS data (Table 1), alkali metal promoters are practically only found on the outer catalyst surface. It is noteworthy that, in general, with such promoters the M/Mo surface ratios are higher than for alkaline earth promoted nickel molybdates. Quantitative XPS analyses showed that, for the Ba-doped catalysts, the M/Mo atomic ratios of promoter are lower than those found by ICP. Moreover, the Ba/Mo surface ratios are practically constant for Ba loadings in the initial solutions higher than 6%. These results suggest the possible formation of barium oxide crystals with size increasing for high Ba loadings, thus decreasing the barium oxide dispersion. Moreover, the crystals block pores of the solid with the subsequent surface area decrease.

The observation of peroxide compounds by XRD only in the barium containing catalysts is not only due to the high promoter concentration (until 12%), but also because in the IIA group barium yields the most stable peroxide (43). The presence of such peroxide compounds in Ba-, Ca-, and Sr-doped samples was found by FTIR (Fig. 3) and in case of Ba-doped samples by FT Raman.

It is important to remind that the alkaline earth-doped catalysts present a decrease in BET surface areas with respect to the unpromoted $NiMoO_4$ (Table 1). However, their surface areas are larger than those exhibited by the alkali promoted samples; in fact, 3% K and 3% Cs–$NiMoO_4$ present the smallest BET areas and the smallest activity (Fig. 8). The catalytic activity is directly affected by the area decrease. We have already reported a decrease of butane conversion with alkali promoted $NiMoO_4$ (21). Similar trends have also been reported for propane ODH on V_2O_5/TiO_2 and MoO_3/TiO_2 catalysts (25) and have been attributed to blocking of alkane activation centers. However, the nature of the promoters also affects the rates of butane conversion (21).

The different catalytic behaviors of alkali and alkaline earth-promoted catalysts can be explained mainly by their different basicities. The larger basicity of alkali metals makes interactions between hydrocarbons and the catalyst surface difficult. Therefore, the butane adsorption is hindered and consequently the rates of butane conversion are lower with K- and Cs-doped $NiMoO_4$. Also the alkali-promoted catalysts present, at equal conversion levels, higher selectivities to C_4 products. This fact was also reported by other authors (13, 21, 25) and is understandable taking into account that the increase of the surface basicity will facilitate the desorption of dehydrogenation products, preventing them from further oxidation to carbon oxides.

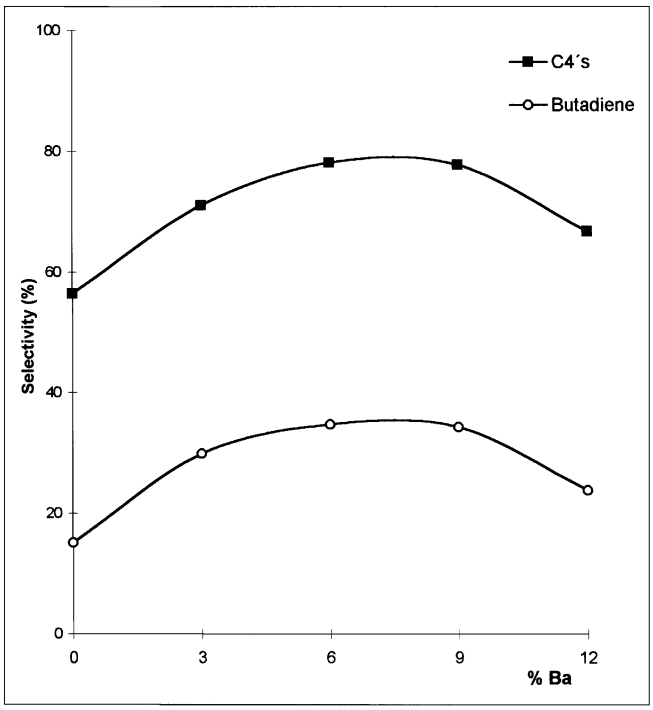

FIG. 12. Influence of barium content on selectivity to dehydrogenation products and butadiene at equal conversion levels (4%) (same reaction conditions as Fig. 8).

Probably, the excessive basicity of alkali-promoted catalysts does not favor subsequent dehydrogenation, and so, these catalysts present smaller butadiene selectivities at equal conversion levels. The lower basicity of alkaline earth-promoted $NiMoO_4$ catalysts must facilitate the adsorption of olefins thus increasing the formation of butadiene.

As suggested by Kung *et al.* for the ODH of light alkanes (26), the first step of the reaction would involve activation of the alkane molecule to form a radical and a surface OH group. It has been proposed that the reaction is initiated by highly reactive surface oxygen species. The selectivity would be determined by the electron density of the oxygen and the position at which the reactive oxygen attacks the surface intermediate.

A reaction that is usually admitted to be performed through a radicalar mechanism is the oxidative coupling of methane. As described by Dissanayake *et al.* (44), different types of metal oxides have been studied for this reaction activating methane via different types of surface oxygen species. In their own work performed with perovskites, they found that BaO_2 is the more active phase for methane oxidative coupling. Sinev *et al.* (45) suggested the formation of CH_3 radicals by the interaction of methane molecules with peroxide ions. For butane as reactant, few papers have been found concerned with the role played by the surface oxygen species in its activation. They are usually related to V–Mg–O (13) and V–P–O (46) systems and nothing was found for Ni–Mo–O.

The results of FTIR, FT Raman, and XRD for alkaline earth-doped $NiMoO_4$ catalysts evidence the existence of new oxygen species, related to alkaline earth oxides and peroxides, not observed in alkali-doped catalysts. It is likely that the catalytic behaviors of the doped nickel molybdate catalysts, namely the aspect of increased butadiene formation, can be related to such oxygen species.

As it was reported in a paper on nickel molybdates doped with different cesium concentrations (33), there is, for the concerned reaction, a close relation between the catalyst basicity and the catalytic behavior, in particular about the selectivity to dehydrogenation products. The increase in promoter contents lead to an increase of the global basicity which cause an increase of the selectivity to C_4's. However, beyond a certain concentration, an overdoping effect was evidenced by the fact that the total basicity does not increase (and even decrease), as showed by the CO_2-TPD results. In such case, the representation of S_{C_4}'s versus promoter contents exhibits a maximum at 3% Cs. A similar behavior was found for barium, with maximum at 9%, either for C_4's selectivity (Fig. 12) or for total adsorbed CO_2 (Fig. 7B), due to its lower basic strength as evidenced by the CO_2-TPD measurements (Fig. 7A).

The detection of O_2^{2-} species in the Ba-doped catalysts was performed by FT Raman and FTIR. Moreover, the FTIR data evidenced that an increase of Ba loading leads to an increase of their characteristic bands intensity (Fig. 4), very pronounced up to 9% of promoter (in surface 4.1%, according to XPS data). A similar behavior was detected in other systems. Lunsford *et al.* (40) found for Ba/MgO catalysts, that contained from 0.5 to 15 mol% Ba, a marked increase in Raman intensity of O_2^{2-} ions in the 2–4 mol% range, with smaller increases at higher loadings. They suggested that a two-dimensional surface phase of BaO/BaO_2 may form at low loadings, and at higher loadings larger crystallites of BaO_2 are formed. Yamashita *et al.* (47) demonstrated that O_2^{2-} ions were present on the surface of Ba/La_2O_3 catalysts, but they found that the catalysts containing larger amounts of barium (which were relatively inactive for CH_4 conversion) presented poor dispersion of O_2^{2-} ions. In this way, according to XPS and ICP data, the formation of a BaO_x surface phase would occur in the doped nickel molybdate catalysts up to 6–9% Ba. At higher loadings the dispersion would be poorer, due to the formation of three-dimensional BaO_x crystallites, leading to a decrease in the amount of adsorbed CO_2.

5. CONCLUSIONS

The addition of alkali and alkaline earth promoters to α-$NiMoO_4$ samples leads to different effects. Using the same preparation procedure and promoter loading, in case of alkaline earth element the nominal content of promoter is found in the catalyst bulk, but for alkali metals such content is found on the surface and only traces are detected in the bulk. However, the physical, chemical, and catalytic effects are more pronounced in case of alkali elements. Both promoters led to a decrease in surface area, influencing in this way the rates of butane conversion. These promoters, however, also affect the surface chemical nature of the $NiMoO_4$ catalysts since new oxygen species were detected in the alkaline earth-doped samples and an increase of basicity was recorded. Alkali-promoted $NiMoO_4$ has a higher basicity that strongly favors the desorption of dehydrogenation products, thus preventing total oxidation. However, subsequent dehydrogenation is also inhibited. Alkaline earth-promoted α-$NiMoO_4$ presents lower basicity. It favors further interaction of reaction intermediates with the catalyst thus increasing butadiene formation and leading to butadiene selectivity about twice of the unpromoted α-$NiMoO_4$, at equal conversion level. This is important due to the great interest of producing butadiene directly from butane. The CO_2-TPD results also evidenced an increase in the basicity of the barium-doped catalysts with the promoter loading up to 9%. However, an overdoping effect was detected and for higher Ba concentrations the basicity decreases. The ICP, XRD, FTIR, FT Raman, and XPS data suggest the formation of three-dimensional BaO_x crystallites at higher Ba contents, which leads to a poorer barium dispersion. These results are in very good agreement

with the maximum for C_4's selectivity observed for the 9% Ba–$NiMoO_4$.

ACKNOWLEDGMENTS

L.M.M. thanks PRAXIS XXI Program of JNICT (Junta Nacional de Investigação Científica e Tecnológica) and F.J.M.H. and R.M.M.A. thank the European Community for financial support. Support of this work by European Community (Contract CHRX-CT92-0065) is gratefully acknowledged. The authors thank Dr. D.M. Nevskaia for the UVDRS measurements and Dr. Miguel A. Bañares for the FT Raman spectra.

REFERENCES

1. McKetta, J. J., "Chemical Processing Handbook." Dekker, New York, 1993.
2. Bielanski, A., and Haber, J., "Oxygen in Catalysts." Dekker, New York, 1991.
3. Wittcoff, H. A., *Chem. Tech.* **20**, 48 (1990).
4. Seshan, K., Swaan, H. M., Smits, R. H. H., Van Ommen, J. G., and Ross, J. R. H., *in* "New Developments in Selective Oxidation" (G. Centi and F. Trifirò, Eds.), Studies in Surface Science and Catalysis, Vol. 55, p. 502. Elsevier, Amsterdam, 1990.
5. Mazzocchia, C., del Rosso, R., and Centola, P., *Ann. Quim.* **79**, 108 (1983).
6. Ozkan, U., and Schrader, G. L., *J. Catal.* **95**, 120 (1985).
7. Ozkan, U., and Schrader, G. L., *J. Catal.* **95**, 137 (1985).
8. Ozkan, U., and Schrader, G. L., *J. Catal.* **95**, 155 (1985).
9. Harding, W. D., Kung, H. H., Kozhevnikov, V. L., and Poeppelmeier, K. R., *J. Catal.* **144**, 597 (1993).
10. Owen, O. S., Kung, M. C., and Kung, H. H., *Catal. Lett.* **12**, 45 (1992).
11. Takita, Y., Tanaka, K., Ichimura, S., Mizihara, Y., Abe, Y., and Ishihara, T., *Appl. Catal. A* **103**, 281 (1993).
12. Huff, M., and Schmidt, L. D., *J. Catal.* **149**, 127 (1994).
13. Chaar, M. A., Patel, D., Kung, M. C., and Kung, H. H., *J. Catal.* **105**, 483 (1987).
14. Busca, G., Lorenzelli, V., Oliveri, G., and Ramis, G., *in* "New Developments in Selective Oxidation II" (V. Cortés Corberán and S. V. Bellón, Eds.), Studies in Surface Science and Catalysis, Vol. 82, p. 253. Elsevier, Amsterdam, 1994.
15. Thompson, M. R., Hess, A. C., Nicholas, J. B., White, J. C., Anchell, J., and Ebner, J. R., *in* "New Developments in Selective Oxidation II" (V. Cortés Corberán and S. V. Bellón, Eds.), Studies in Surface Science and Catalysis, Vol. 82, p. 167. Elsevier, Amsterdam, 1994.
16. Overbeek, R. A., Versluijs-Helder, M., Warringa, P. A., Bosma, E. J., and Geus, J. W., *in* "New Developments in Selective Oxidation II" (V. Cortés Corberán and S. V. Bellón, Eds.), Studies in Surface Science and Catalysis, Vol. 82, p. 183. Elsevier, Amsterdam, 1994.
17. Kubias, B., Meised, M., Wolf, G. U., and Rodemerck, U., *in* "New Developments in Selective Oxidation II" (V. Cortés Corberán and S. V. Bellón, Eds.), Studies in Surface Science and Catalysis, Vol. 82, p. 195. Elsevier, Amsterdam, 1994.
18. Finocchio, E., Busca, G., Lorenzelli, V., and Willey, R. J., *J. Catal.* **151**, 204 (1995).
19. Burrington, J. D., Kartisek, C. T., and Grasselli, R. K., *J. Catal.* **63**, 235 (1980).
20. Mazzocchia, C., Aboumrad, C., Diagne, C., Tempesti, E., Herrmann, J. M., and Thomas, G., *Catal. Lett.* **10**, 181 (1991).
21. Martín-Aranda, R. M., Portela, M. F., Madeira, L. M., Freire, F., and Oliveira, M., *Appl. Catal. A* **127**, 201 (1995).
22. Driscoll, S. A., Gardner, D. K., and Ozkan, U. S., *J. Catal.* **147**, 379 (1994).
23. Mamedov, E. A., *Catal. Rev. Sci. Eng.* **36**, 1 (1994).
24. Grzybowska, B., Mekss, P., Grabowski, R., Waislo, K., Barbaux, Y., and Gengembre, L., *in* "New Developments in Selective Oxidation II" (V. Cortés Corberán and S. V. Bellón, Eds.), Studies in Surface Science and Catalysis, Vol. 82, p. 151. Elsevier, Amsterdam, 1994.
25. Grabowski, R., Grzybowska, B., Samson, K., Sloczynski, J., Stoch, J., and Wcislo, K., *Appl. Catal. A* **125**, 129 (1995).
26. Kung, H. H., Michalakos, P., Owens, L., Kung, M., Andersen, P., Owen, O., and Jahan, I., *in* "Catalytic Selective Oxidation" (S. T. Oyama and J. W. Hightower, Eds.), ACS Symposium Series, Vol. 523, p. 389. Am. Chem. Soc., Washington, DC, 1993.
27. Busca, G., and Lorenzelli, V., *J. Chem. Soc. Faraday Trans.* **88**, 2783 (1992).
28. Jiarwen da, Xuejia Ding, and Shikong Shen, *Appl. Catal. A* **116**, 81 (1994).
29. Korf, S. J., Roos, J. A., Derksen, J. W. H. C., Vreeman, J. H., Van Ommen, J. G., and Roos, J. R. H., *Appl. Catal.* **59**, 291 (1990).
30. Lang Ji, Jursheng Lin, Chongya Lin, and Xiancheng Chen, *Appl. Catal. A* **114**, 207 (1994).
31. Ueda, W., Young-Seek Yoon, Fujikawa, N., Kyu-Wan Lee, and Moro-oka, Y., *in* "Proceedings, EUROPACAT-II, Maastricht, 1995," p. 96.
32. Dingjun Wang, Rosynek, M. P., and Lunsford, J. H., *J. Catal.* **151**, 155 (1995).
33. Maldonado-Hódar, F. J., Madeira, L. M., Portela, M. F., Martín-Aranda, R. M., and Freire, F., *J. Mol. Catal. A* **111**, 313 (1996).
34. Plyasova, L. M., Ivanchenko, I. Yu., Andrushkevich, M. M., Buyanov, R. A., Itenberg, I. Sh., Khramova, G. A., Karakchiev, L. G., Kustova, G. N., Stepanov, G. A., Tsailingol'd, A. L., and Pilipenko, F. S., *Kinet. Catal.* **14**, 1010 (1973).
35. Cross, A. D., and Alan Jones, R., "An Introduction to Practical Infra-Red Spectroscopy." Butterworths, London, 1969.
36. Davydov, A. A., "Infrared Spectroscopy of Adsorbed Species on the Surface of Transition Metal Oxides." Wiley, Chichester, 1990.
37. Williams, C. C., Ekerdt, J. G., Jehng, J., Hardcastle, F. D., Turek, A. M., and Wachs, I. E., *J. Phys. Chem.* **95**, 8781 (1991).
38. Jin, Y. S., Auroux, A., and Vedrine, J. G., *J. Chem. Soc. Faraday Trans.* **85**, 4179 (1989).
39. Walrafen, G. E., Krishnan, P. N., Hokmabadi, M., Griscom, D. L., and Munro, R. G., *J. Chem. Phys.* **77**, 3840 (1982).
40. Lunsford, J. H., Yang, X., Haller, K., and Laane, J., *J. Phys. Chem.* **97**, 13810 (1993).
41. Su, S. C., and Bell, A. T., *Catal. Lett.* **36**, 15 (1996).
42. Fournier, J., Louis, C., Che, M., Chaquin, P., and Masure, D., *J. Catal.* **119**, 400 (1989).
43. Heslop, R. B., and Jones, H., "Química Inorgânica." Fundação Calouste Gulbenkian, Lisboa, 1988.
44. Dissanayake, D., Kharas, K. C. C., Lunsford, J. H., and Rosynek, M. P., *J. Catal.* **139**, 652 (1993).
45. Sinev, M. Y., Korchak, V. N., and Krylov, O. V., *Kinet Katal.* **27**, 1274 (1986).
46. Cavani, F., and Trifirò, F., *in* "Catalysis Vol. 11," Specialist Periodical Reports, p. 246. Royal Chem. Soc. Cambridge, 1994.
47. Yamashita, H., Machida, Y., and Tomita, A., *Appl. Catal.* **79**, 203 (1991).